Article type: Research Article

Received Jun. 25, 2020

Accepted Oct. 15, 2020

Edited by: Suomeng Dong, Nanjing Agricultural University, China

Running title: AtANN8 negatively regulates RPW8.1

ANNEXIN 8 negatively regulates RPW8.1-mediated cell death and disease resistance in *Arabidopsis*

Zhi-Xue Zhao[1,3], Yong-Ju Xu[1,3,4], Yang Lei[1,3,5], Qin Li[1,3,6], Ji-Qun Zhao[1], Yan Li[1], Jing Fan[1], Shunyuan Xiao[2], Wen-Ming Wang[1*]

[1]Rice Research Institute and Key Laboratory for Major Crop Diseases, Sichuan Agricultural University, Chengdu 611130, China.

[2]Institute for Bioscience and Biotechnology Research & Department of Plant Science and Landscape Architecture, University of Maryland, Rockville, MD 20850, USA.

[3]These authors contributed equally to the paper.

[4]Present address: Industrial Crop Research Institue, Sichuan Academy of Agricultural Science, Chengdu 610300, China.

This article has been accepted for publication and undergone full peer review but has not been through the copyediting, typesetting, pagination and proofreading process, which may lead to differences between this version and the Version of Record. Please cite this article as doi: 10.1111/jipb.13025.

[5]Present address: Guangyuan Tobacco Company Wangcang Branch, Guangyuan 628200, China.

[6]Present address: Plant Protection Station of Pingchang County, Bazhong 636400, China.

*Corresponding author: Wen-Ming Wang (j316wenmingwang@sicau.edu.cn)

Abstract

Study on the regulation of broad-spectrum resistance is an active area in plant biology. *RESISTANCE TO POWDERY MILDEW 8.1* (*RPW8.1*) is one of a few broad-spectrum resistance genes triggering the hypersensitive response (HR) to restrict multiple pathogenic infections. To address the question how RPW8.1 signaling is regulated, we performed a genetic screen and tried to identify mutations enhancing RPW8.1-mediated HR. Here, we provided evidence to connect an annexin protein with RPW8.1-mediated resistance in *Arabidopsis* against powdery mildew. We isolated and characterized *Arabidopsis b7-6* mutant. A point mutation in *b7-6* at the *At5g12380* locus resulted in an amino acid substitution in ANNEXIN 8 (AtANN8). Loss-of-function or RNA-silencing of *AtANN8* led to enhanced expression of *RPW8.1*, RPW8.1-dependent necrotic lesions in leaves, and defense against powdery mildew. Conversely, over-expression of *AtANN8* compromised RPW8.1-mediated disease resistance and cell death. Interestingly, the mutation in AtANN8 enhanced RPW8.1-triggered H_2O_2. In addition, mutation in AtANN8 led to hypersensitivity to salt stress. Together, our data indicate that AtANN8 is involved in multiple stress signaling pathways and negatively regulates RPW8.1-mediated resistance against powdery mildew and cell death, thus linking ANNEXIN's function with plant immunity.

Keywords: AtANN8, Cell death, Disease resistance, H_2O_2, Hypersensitive response, Powdery mildew, RPW8.1

INTRODUCTION

Plants have evolved an innate immune system, which consists of two tiers to protect themselves against invading pathogens (Jones and Dangl 2006; Zhou and Zhang 2020). The first tier, termed as pathogen-associated molecular pattern (PAMP)-triggered immunity (PTI), is activated upon recognition of evolutionarily conserved PAMPs by cell surface pattern-recognition receptors (PPRs) (Dodds and Rathjen 2010). Defense responses activated during PTI include increase in ion fluxes, such as Ca^{2+} fluxes, phosphorylation events, such as mitogen-activated protein kinase (MAPK) signaling cascades activation and Ca^{2+}-dependent protein kinases activation, reactive oxygen species (ROS) production, transcriptional reprogramming, changes in hormone concentrations, and callose deposition (Bittel and Robatzek 2007; Seybold et al. 2014). These responses form a signaling network that can successfully ward off most potential pathogens. Adapted pathogens employ a suite of effectors to subvert PTI and facilitate colonization (Dou and Zhou 2012). To fight against such pathogens, plants activate the second layer of immune system through recognition of the specific effectors by plant resistance (R) proteins. Defense responses activated during effector-triggered immunity (ETI) are much stronger than those during PTI (Li et al. 2013). Conceivably, PTI and ETI are evolutionarily interconnected, with PTI being the major contributor to pre-invasion defense, and both of them being responsible for effective post-invasive defense.

Most characterized plant *R* genes encode the nucleotide-binding site-leucine-rich repeat (NB-LRR) receptors each of which is activated upon recognition of a cognate effector (Dangl et al. 2013). A few genetically defined *R*

genes encoding non-NLR proteins are also capable of activating similar defense responses, including bursts of ROS, up-regulation of defense-related genes and callose deposition. For example, *REACTION TO PUCCINIA GRAMINIS1* (*Rpg1*) from barley (*Hordeum vulgare*) encodes a receptor-like kinase and activated by the concerted action of two effectors (Brueggeman et al. 2002; Nirmala et al. 2011). *LEAF RUST RESISTANCE 34* (*Lr34*) from wheat encodes an ATP-binding cassette (ABC) transporter and confers resistance to multiple pathogens in wheat and transgenic barley (Krattinger et al. 2009; Risk et al. 2013). *Arabidopsis RESISTANCE TO POWDERY MILDEW 8.1* (*RPW8.1*), as well as *RPW8.2*, encodes small basic protein with limited homology to the coiled-coil domain of some NLR proteins and confer the broad-spectrum resistance against powdery mildew (Xiao et al. 2001). Those RPW8 domain-containing NLRs (such as NRG1 and ADR1) have recently been shown to play a critical role in defense signaling activated by multiple effector-sensing NLRs (Castel et al. 2019; Wu et al. 2019).

RPW8.1 and RPW8.2 share 65% similarity and 45% identity in amino acid sequences. The *RPW8.2* expression is induced by the powdery mildew infection through a salicylic acid (SA)-dependent feedback circuit and the RPW8.2 is specifically targeted to extra-haustorial membrane (EHM) that encases the fungal feeding structure named haustorium (Xiao et al. 2003; Wang et al. 2009). While adequate expression and accurate localization of RPW8.2 is critical for activation of defense responses (Wang et al. 2010; Huang et al. 2019), also RPW8.2 is under negative regulation presumably for minimizing the cost-of-resistance associates with expression of RPW8.1 and RPW8.2 in absence of the pathogens (Orgil et al. 2007). Indeed, genetic screens identified an inositol phosphorylceramide synthase as a negative regulator for RPW8.2-mediated disease resistance and cell death (Wang et al. 2008). Yeast-two-hybridization screens also identified a protein phosphatase type 2 C (i.e. PAPP2C) as a negative regulator of RPW8.2-mediated

disease resistance and cell death (Wang et al. 2012). The function of RPW8.1 is distinguishable from that of RPW8.2 both in terms of subcellular localization and the capability of triggering cell death. RPW8.1 is localized to ring structures surrounding the chloroplasts in the mesophyll cells and promotes hypersensitive response (HR)-like cell death and the basal defense against different pathogens when expressed by its native promoter (Ma et al. 2014; Li et al. 2018). However, how the function of RPW8.1 is regulated remains an open question.

ANNEXINs are multifunctional small proteins capable of Ca^{2+}-dependent membrane binding or membrane insertion, and linking Ca^{2+}, lipid signaling and redox to regulation of development and responses to environmental stimuli (Gerke et al. 2005). Members of ANNEXINs are involved in diverse biological functions in prokaryotes and eukaryotes, including actin binding, exocytosis, peroxidase activity, ion transport and callose synthase regulation (Laohavisit and Davies 2011). For example, in animal cells, ANNEXIN V can be used as an apoptosis marker to detect the cells that have expressed phosphatidylethanolamine (PE) and phosphatidylserine (PS) on cell surface, which is an event found in apoptosis (Meers and Mealy 1994). In plants, ANNEXINs have been shown to be involved in the H_2O_2-activated Ca^{2+} fluxes (Konopka-Postupolska et al. 2009; Laohavisit et al. 2010), act as the Ca^{2+}-permeable transporters (Laohavisit et al. 2009), or exhibit peroxidase activity (Gidrol et al. 1996; Laohavisit et al. 2009). Not surprisingly, some plant ANNEXINs have been suggested to play roles in response to various abiotic stresses (Gorantla et al. 2005; Espinoza et al. 2017), and biotic stresses (Jami et al. 2008; Zhou et al. 2013). However, whether ANNEXINs play roles in plant immunity has not been definitely characterized.

In order to investigate how *RPW8.1* might be distinctly regulated, we conducted a genetic screen to identify the mutations that enhanced or compromised

RPW8.1-mediated spontaneous HR-like cell death. Previously, we reported that proper expression of the MYB domain transcription factor ASYMMETRIC LEAVES 1 (AS1) is required for RPW8.1-mediated resistance against powdery mildew (Zhao et al. 2015). Here, we added the isolation and characterization of another mutant, *b7-6* from the same genetic screen. This mutant contains a nonsynonymous mutation in an ANNEXIN family member, *AtANN8* (*At5g12380*) and exhibits enhanced RPW8.1-mediated spontaneous HR-like cell death. Our results indicate that AtANN8 negatively regulates RPW8.1-mediated disease resistance and cell death, providing genetic evidence for the involvement of a particular ANNEXIN in regulation of plant immunity.

RESULTS

Isolation and cloning of *b7-6*

We obtained the mutant *b7-6* in a genetic screen in R1Y4 background. R1Y4 is one Col-gl (the glabrous mutation in Col-0 background) transgenic line that ectopically expresses RPW8.1-YFP from its native promoter conferring resistance to downy mildew and virulent powdery mildew pathogens (Ma et al. 2014). The transgenic line was used in the functional investigation because RPW8.1 is tandemly arrayed with RPW8.2 in *Arabidopsis* accession Ms-0, and Col-0 lacks both *RPW8.1* and *RPW8.2* (Xiao et al. 2001). Any observed phenotypes different from Col-0 in the transgenic line would be due to the results of ectopic expression of the transgene. To understand the genetic basis of RPW8.1-mediated broad-spectrum resistance, we mutagenized seeds of the homozygous R1Y4 line using ethyl methanesulfonate (EMS) and screened for mutants with spontaneous cell death phenotypes. In present study, we added the isolation and characterization of the mutant *b7-6* that showed spontaneous HR-like cell death (SHL) in mature leaves in absence of any pathogen (Figure 1A, B). We mapped

the mutation to chromosome 5 between two SSLP markers T22P22 and T24H18 by using an F_2 population derived from *b7-6* × Ler (Figure S1A). By sequencing the genes in this region in *b7-6*, we identified a single G-to-A point mutation in one ANNEXIN family member *AtANN8* (*At5g12380*) that results in a substitution of Ala at position 94 to Thr (Figure 1C, D, and Figure S1A). Alignment of sequence homologs of ANN8 from different organisms showed that the A94 site is highly conserved (Figure 1E), implying that this residue is critical for the function of AtANN8 and its orthologs in various organisms. To determine if this mutation is responsible for the mutant phenotype, we obtained more than 20 transgenic lines expressing the wild type *AtANN8* gene or the *AtANN8-YFP* fusion gene, respectively, from the native promoter in *b7-6* and observed the disappearance of the spontaneous HR-like cell death of *b7-6* (Figure 1F), indicating that the A94T mutation in AtANN8 is responsible for the enhanced cell death phenotype observed in *b7-6*. We thus renamed *b7-6* as R1Y4/*ann8-1* and *b7-6* transgenic line expressing the wild type *AtANN8* gene as R1Y4/*ann8-1*/ANN8.

AtANN8 is rapidly and transiently induced by pathogen challenge

The *Arabidopsis* ANNEXIN protein family contains eight members (Figure S1C). AtANN1 was reported and involved in stress response and might act as Ca^{2+} channel (Laohavisit et al. 2012; Richards et al. 2014). However, biological functions for the other members remain unknown even though transcript levels of some members displayed changes upon pathogen attack based on high-throughput expression data (Wang et al. 2005; Truman et al. 2007; Chandran et al. 2010). We thus first examined the expression of all the family members, except *AtANN6* (which failed to amplify), in uninfected stem, inflorescence (flower) and leaf tissues, as well as in powdery mildew-infected leaves. While *AtANN1*, *AtANN3*,

AtANN5 and *AtANN7* were expressed at low levels in all tissues examined, *AtANN4* and *AtANN8* particularly displayed preferential expression in leaves (Figure 2A). More interestingly, expression of *AtANN2* and *AtANN8* but not *AtANN4* was up-regulated in powdery mildew infected leaves, with *AtANN8* being the highest expressor (Figure 2A). To further assess which ANNEXIN family members respond to biotic stress, we examined the expression of *AtANN1*, *AtANN2*, *AtANN4* and *AtANN8* in response to leaf inoculation from three different *Pseudomonas syringae* pv. *Tomato* (*Pst*) strains (Figure 2B-E). *AtANN1*, *AtANN2*, and *AtANN4* were all more or less up-regulated in both mock- and *Pst*-inoculated leaves, suggesting that these three genes may be responsive to both biotic and abiotic stresses as previously reported (Konopka-Postupolska et al. 2009; Huh et al. 2010), as well as to mechanical wounding induced by leaf infiltration in this study. By contrast, *AtANN8* did not respond to wounding, but showed strong induction in response to challenges from different *P. syringae* strains with distinct kinetics. In leaves inoculated with the virulent strain *Pst* DC3000, *AtANN8* was highly expressed at 24 hpi and then dropped ~3-fold at 48 hpi (Figure 2E). Upon inoculation of the avirulent strain *Pst AvrRpm1*, *AtANN8* was highly induced at 3 hpi and then dropped to the background level at later time points. However, in leaves inoculated with the non-pathogenic strain *Pst hrcC*$^{-}$, *AtANN8* was only slightly up-regulated at 48 hpi (Figure 2E). Combined, these data suggest that *AtANN8* may be more specifically involved in response to biotic stress than other ANNEXIN family members.

Because *AtANN8* expression is particularly responsive to bacterial challenge, we tested if the A94T mutation in *AtANN8* affects defense against bacterial pathogens. To this end, we obtained a Col-gl line containing *ann8-1* in the absence of the *RPW8.1* transgene from the offspring of the cross between R1Y4/*ann8-1* and Col-gl. The Col-gl/*ann8-1* line (referred to as *ann8-1* hereafter) did not exhibit

any necrotic lesion phenotype (Figure 3A), implying that the necrotic lesions in R1Y4/*ann8-1* is RPW8.1-dependent. Because R1Y4 supported significantly less growth of the virulent bacterial strain *Pst* DC3000 but not the avirulent strains (Li et al. 2018), we examined whether the mutation in *AtANN8* leads to any change in response to *Pst* DC3000. Our results showed that *ann8-1* supported bacterial growth similar to Col-gl, while R1Y4/*ann8-1* supported significantly less bacterial growth than Col-gl, but similar to R1Y4 (Figure 3B). These data indicated that the A94T mutation in AtANN8 might not affect plant defense against virulent bacterial strain, although *AtANN8* expression is responsive to bacterial challenge.

Knocking-down *AtANN8* by artificial microRNA leads to RPW8.1-dependent cell death

To confirm *AtANN8* is functionally connected to *RPW8.1*, we employed artificial microRNA that specifically targets *AtANN8* (*amiRANN8*) to knock down its expression following WMD Web MicroRNA Designer (http://wmd3.weigelworld.org). We first obtained more than 20 *amiRANN8* transgenic lines in the Col-gl background but did not observe any obvious phenotype from any of these lines (Figure 3C). We checked the expression level of *AtANN8* in four representative lines to assess if the *amiRANN8* transgene worked. The expression levels of *AtANN8* in the four *amiRANN8* lines were less than 20% of that in Col-gl as measured by reverse transcription quantitative PCR (RT-qPCR) (Figure 3D), indicating that *amiRANN8* did work to silence *AtANN8*. However, when we crossed three *amiRANN8* transgenic lines with R1Y4, we observed cell death lesions in all F_1 plants and the F_2 individuals expressing both the *RPW8.1-YFP* and the *amiRANN8* transgenes from any of the three RNAi lines (Figure 3E). Thus, genetic depletion of *AtANN8* by RNAi produced similar effect as the *ann8-1* mutation in enhancing RPW8.1-YFP-dependent HR-like cell death.

Together, these data indicate that *AtANN8* genetically acts as a negative regulator of RPW8.1-mediated cell death.

Impairment of AtANN8 enhances RPW8.1 expression

We previously observed that ectopic expression of *RPW8.1* did not lead to obvious cell death lesions (Ma et al. 2014). Occurrence of cell death lesions in R1Y4/*ann8-1* but not in *ann8-1* prompted us to examine if cell death is due to enhanced expression of *RPW8.1*. Under Laser Scanning Confocal Microscopy (LSCM), only a small number of clustered mesophyll cells accumulated RPW8.1-YFP in the fully expanded leaves of 6-week-old R1Y4 plants (Figure 4A). By contrast, almost all mesophyll cells highly expressed RPW8.1-YFP in leaves of R1Y4/*ann8-1* (Figure 4B); and similar high-level accumulation of RPW8.1-YFP was also observed in R1Y4/*amiRANN8-3* (Figure 4C) at the same age. Quantification of the signal intensity of YFP showed that RPW8.1-YFP levels in R1Y4/*ann8-1* and R1Y4/*amiRANN8-3* were about 3-fold of that in R1Y4 (Figure 4D, E). Also, a western blot assay showed that the protein levels of RPW8.1-YFP were higher in R1Y4/*ann8-1* and R1Y4/*amiRANN8-3* than in R1Y4 (Figure S2). Further RT-qPCR analysis showed that *RPW8.1-YFP* was expressed at eleven and five times higher in R1Y4/*ann8-1* and R1Y4/*amiRANN8-3* than in R1Y4 (Figure 4D, E), respectively. These observations indicated that *AtANN8* negatively regulate *RPW8.1* expression at the transcriptional level and possibly the post-transcriptional level.

Impairment of AtANN8 enhances RPW8.1-mediated defense responses

Because R1Y4 exhibited resistance to powdery mildew (Ma et al. 2014), the enhanced necrotic lesions observed in R1Y4/*ann8-1* prompted us to check if mildew resistance of this mutant was further increased. Thus, we inoculated the

powdery mildew strain *Golovinomyces cichoracearum* USCS1 on 6-week-old plants and scored the disease phenotypes. While fungal mass in R1Y4 was obviously less than that in Col-gl control plants, it was hardly visible in R1Y4/*ann8-1* and R1Y4/*amiRANN8-3* plants, indicating enhanced resistance (Figure 4F). However, fungal mass in *ann8-1* and *amiRANN8-3* was comparable with that in Col-gl, indicating no resistance (Figure 4F). Further disease quantification showed that while R1Y4 displayed reduced sporulation by ~2.5-fold compared to Col-gl, R1Y4/*ann8-1* and R1Y4/*amiRANN8-3* rarely supported fungal sporulation (Figure 4G). These observations support negative regulation of *RPW8.1*-dependent resistance against powdery mildew by *AtANN8*.

Next, we examined the expressions of the defense-related genes, *PR1* and *FRK1* that acts as marker genes for SA-signaling and PTI, respectively. Both of these genes were up-regulated during powdery mildew invasion and reached a peak at 7 dpi in R1Y4 and R1Y4/*ann8-1* (Figure 4H, I). Compared with R1Y4, R1Y4/*ann8-1* showed significantly enhanced *FRK1* expression at 7 and 10 dpi (Figure 4H), and *PR1* expression at 2, 4, 7 and 10 dpi (Figure 4I), suggesting that the enhancement of RPW8.1-mediated defense activation by functional impairment of AtANN8 upon powdery mildew challenge may be attributable to elevated PTI and SA-signaling.

Because plant defense against powdery mildew is often associated with cell death, we examined host cell death by trypan blue staining of the leaves free or at 10 dpi of powdery mildew. In the absence of pathogen, Col-gl and *ann8-1* did not have any cell death, whereas both R1Y4/*ann8-1* and R1Y4/*amiRANN8-3* displayed more clusters of dead cells than R1Y4, but R1Y4/ann8-1/ANN8 had cell death similar to that in R1Y4 (Figure 5A, B), confirming that functional impairment of *AtANN8* results in RPW8.1-YFP–dependent leaf cell death

independent of pathogen challenge. After powdery mildew pathogen infection, cell death in Col-gl and *ann8-1* mutant was rarely if ever detectable, while cell death in R1Y4/*ann8-1* and R1Y4/*amiRANN8-3* were further increased compared to that in R1Y4 (Figure 5C, D). These data indicate that functional impairment in AtANN8 enhances RPW8.1-dependent cell death, which could further increase RPW8.1-mediated powdery mildew resistance.

Because cell death triggered by RPW8.1 and RPW8.2 is preceded by H_2O_2 production (Xiao et al., 2003), we wondered whether H_2O_2 production and distribution in R1Y4/*ann8-1* was different from that of R1Y4. To this end, we examined H_2O_2 accumulation by 3,3'-Diaminobenzidine (DAB) staining at 2 dpi of *G. cichoracearum* USCS1. Consistent with a previous report (Ma et al. 2014), R1Y4 showed H_2O_2 accumulation in the apoplastic space between mesophyll cells (Figure 5E, F). By contrast, H_2O_2 in R1Y4/*ann8-1* was mainly found inside chloroplasts of some mesophyll cells (Figure 5G) and in unknown compartments between mesophyll cells (arrows in Figure 5H). These observations indicate that site of H_2O_2 accumulation triggered by RPW8.1 in mesophyll cells is altered when AtANN8 is functionally impaired, further suggesting that RPW8.1 may positively regulate H_2O_2 production in mesophyll cells.

Over-expression of AtANN8 compromises RPW8.1-mediated cell death and disease resistance

Since both the A94T mutation and knocking-down of *AtANN8* could enhance RPW8.1-mediated defense response and cell death, we wondered if over-expression of *AtANN8* could inhibit RPW8.1's function. To this end, we obtained transgenic plants expressing *AtANN8* from the *35S* promoter in Col-gl (*ANN8OE*) and R1Y4 (R1Y4/*ANN8OE*). While more than 15 transgenic *ANN8OE* lines did not show any obvious phenotype, eight transgenic R1Y4/*ANN8OE* lines

showed leaf phenotypes similar to that of wild type (Figure 6A), indicating compromised RPW8.1-mediated cell death. Further RT-qPCR analysis showed that the *AtANN8* transgene was indeed highly expressed in all examined *ANN8OE* lines compared to the mRNA level of the endogenous *AtANN8* gene in Col-gl (Figure 6B). Meanwhile, the expression of *RPW8.1-YFP* was significantly suppressed in the R1Y4/*ANN8OE* lines (Figure 6C). We then examined powdery mildew resistance in these lines. Not surprisingly, both R1Y4/*ANN8OE-1* and R1Y4/*ANN8OE-2* were more susceptible to powdery mildew than R1Y4 even though they were slightly less susceptible compared with Col-gl or a Col-gl line transgenic for *35S::AtANN8* (*ANN8OE*) (Figure 6D). These phenotypes were validated by spore quantification (Figure 6E). Taken together, these results reinforce the idea that *AtANN*8 negatively regulates *RPW8.1*-mediated disease resistance and cell death through mechanisms that include suppression of *RPW8.1* expression.

AtANN8 is involved in abiotic stress responses and associates with ER/endomembrane in the cytoplasm

ANNEXINs have been involved in Ca^{2+}-signaling (Laohavisit et al. 2010) and some family members such as AtANN1 and OsANN1 have been shown to be implicated in the abiotic stress responses (Richards et al. 2014; Qiao et al. 2015). To examine if AtANN8 also plays a role in abiotic stress responses, we first tested seedlings under different salt concentrations. When grown in MS-agar containing 100 mM NaCl, *ann8-1* and *amiRANN8-3* generated shorter roots than Col-gl (Figure 7A, B), indicating hypersensitivity to NaCl. This result implied that AtANN8 may play a role in osmosis across cell membrane in response to salt stress. By contrast, we observed no significant differences in root length when seedlings were grown in MS-agar containing 10 μM JA or 0.1 M H_2O_2 (Figure

7B). Intriguingly, *ann8-1* seedlings seemed to have longer roots than Col-gl and *amiRANN8-3* when grown in control MS-agar, though not statistically significant. However, the difference became statistically significant when seedlings were grown in MS-agar containing 10 μM SA (Figure 7A, B). The implication of this phenotype for *ann8-1* is currently unknown and will be a future research focus.

Finally, we examined the subcellular localization of AtANN8, in order to understand how AtANN8 regulates RPW8.1 function and abiotic stress responses. We first made and introduced a DNA construct in which AtANN8 was translationally fused with YFP at the C-terminus of AtANN8 under control of the *AtANN8* native promoter in R1Y4/*ann8-1*. The transgenic plants showed phenotypes similar to that of R1Y4, indicating that AtANN8-YFP is functional (Figure 1F). Confocal imaging showed that although YFP signal was mainly detected along the plasma membrane of the epidermal cells, it was also found in intracellular structures (Figure 8A). To further determine the subcellular localization of AtANN8-YFP, we transiently co-expressed it with an RFP nuclear marker obtained in a previous investigation (Huang et al. 2014) in leaves of *Nicotiana benthamiana*. While RFP signal from the nuclear marker was exclusively found in the nucleus, YFP signal from AtANN8-YFP was seen in the cytoplasm with strong signal visible around the nucleus as a typical ER ring (Figure S3). To further validate whether AtANN8-YFP has a co-localization with ER, we co-expressed AtANN8-YFP with the ER marker RFP-HDEL in *N. benthamiana* leaves. As showed in Figure 8B and C, AtANN8-YFP signal looks largely overlapping with RFP signal, however, the YFP signal in Figure 8C is diffuse when comparing to the sharp ER filaments, suggesting that AtANN8-YFP associates with ER in the cytoplasm. To exclude the possibility that a small pool of AtANN8 may colocalize and interact with RPW8.1, we performed a co-immunoprecipitation (Co-IP) assay. The result showed that these two proteins

do not have physical association (Figure S4), suggesting that AtANN8 exerts its regulation on RPW8.1 indirectly.

DISCUSSION

In this study, we obtained genetic and molecular evidence to show that *AtANN8* encoding a putative ANNEXIN protein functions as a negative regulator of the broad-spectrum disease resistance gene *RPW8.1* in *Arabidopsis* in terms of activation of cell death and resistance against powdery mildew. Intriguingly, we also found that the A94T mutation in AtANN8 resulted in RPW8.1-dependent H_2O_2 production and accumulation in the chloroplasts of the mesophyll cells, which is in sharp contrast to the apoplastic H_2O_2 accumulation in the parental line expressing RPW8.1-YFP. How exactly AtANN8 regulates RPW8.1's function is currently unclear but several possible mechanisms can be envisioned given the known diverse cellular functions of some ANNEXINs from *Arabidopsis*, other plant species or non-plant organisms.

AtANN8 might be preferentially engaged in regulation of plant-pathogen interaction

There are eight genes encoding ANNEXINs in *Arabidopsis* genome, of which *AtANN1* is so far the best characterized. Partially purified AtANN1 showed peroxidase activity as it could complement the Δ*oxyR Escherichia coli* mutant by reducing H_2O_2 levels, allowing the mutant bacteria to survive oxidative stress (Gidrol et al. 1996). Genetic studies showed that *AtANN1* is indeed involved in regulating root epidermal $[Ca^{2+}]_{cyt}$ response to the extracellular H_2O_2 because peroxide-stimulated $[Ca^{2+}]_{cyt}$ elevation was aberrant in roots and the root epidermal protoplasts of an *AtANN1* knockout mutant (Richards et al. 2014). Over- or down-expression of *AtANN1* resulted in hyper-or hypo-sensitivity to

drought with reduced or increased accumulation of H_2O_2 in guard cells, respectively (Konopka-Postupolska et al. 2009). Recently, AtANN1 is found to response to heat stress and thus cytoplasmic calcium concentration may be involved in plant endurance to heat stress (Wang et al. 2015). Therefore, AtANN1 is a component of H_2O_2/Ca^{2+} signaling network of plants (Laohavisit et al. 2012; Richards et al. 2014).

In addition to AtANN1, transcriptional changes in response to abiotic or biotic stresses are also reported for the other *Arabidopsis* ANNEXINs. Upon plant exposure to H_2O_2, expression of *AtANN1* (Konopka-Postupolska et al. 2009) and *AtANN2* was found to be declined, while expression of *AtANN3*, *AtANN4*, and *AtANN7* increased, and expression of *AtANN8* remained unchanged (Richards et al. 2014), indicating that different *AtANNs* act differentially in response to oxidative stress. Root-colonization of *Pseudomonas flseudomona*, an rhizosphere beneficial bacterium, resulted in down-regulation of *AtANN3* and *AtANN4* (Wang et al. 2005), while leaf infection by pathogenic *Pseudomonas syringae* induced up-regulation of *AtANN4* (Truman et al. 2007). More interestingly, using laser micro-dissected tissue, *AtANN1* was found to be highly up-regulated at the infection site of the host-adapted powdery mildew species *Golovinomyces orontii* (Chandran et al. 2010). However, whether those *AtANNs* are involved in plant defense remains uncharacterized.

In the present study, we identified AtANN8, by genetic screens, to be functionally connected to RPW8.1 in controlling H_2O_2 accumulation, cell death activation and resistance to powdery mildew. Our genetic data were well corroborated with gene expression analysis: among seven of the eight ANNEXIN genes examined, *AtANN8* was the outstanding family member that showed up-regulation by powdery mildew (at 10 dpi) or transient up-regulation by *P.*

syringae with the peak time being different for the avirulent (3 hpi) and virulent (24 hpi) strains (Figure 2). Thus, it appears that among the eight family members *AtANN8* is more specifically engaged in regulation of plant-pathogen interaction.

AtANN8 may manipulate the distribution of RPW8.1-trigerred H_2O_2

How could AtANN8 be engaged for regulating RPW8.1's function? Our genetic data showed that the *ann8-1* mutation-triggered RPW8.1-YFP-dependent spontaneous HR-like lesions and enhanced mildew resistance correlated with both transcriptional up-regulation and protein accumulation of RPW8.1 (Figure 3 and 4). Conversely, over-expression of *AtANN8* appeared to lower expression of *RPW8.1* and RPW8.1-mediated resistance to powdery mildew (Figure 6). Hence, *AtANN8* negatively regulates *RPW8.1*'s transcription and/or RPW8.1 protein accumulation.

But how could this regulation be realized? Our observations that there was a striking difference in the distribution of RPW8.1-triggered H_2O_2 in leaf tissues of R1Y4 and R1Y4/*ann8-1* imply a potential important mechanistic insight into the RPW8.1-ANN8 relationship. Previously, we demonstrated that RPW8.1 as an R protein is able to trigger H_2O_2 production (Xiao et al. 2003), and the H_2O_2 produced in R1Y4 is frequently detected in the apoplastic space between mesophyll cells and between a mesophyll cell and the above powdery mildew-invaded cell (Ma et al., 2014). However, where the H_2O_2 is produced still remains unknown. RPW8.1-YFP is localized to the membrane ring structures surrounding the chloroplasts in the mesophyll cells (Wang et al., 2007) or in membrane-like structures surrounding stromules protruding from plastids when RPW8.1-YFP is expressed by the *RPW8.2* promoter in epidermal cells (Wang et al., 2013). These earlier observations imply that RPW8.1 may stimulate H_2O_2 production in chloroplasts. If so, H_2O_2 has to be transported out from chloroplasts

into the cytosol and then from the cytosol to the apoplastic space. Because H_2O_2 in R1Y4/*ann8-1* almost exclusively accumulated inside the mesophyll cells with particular enrichment in the chloroplasts (Figure 5G, H), one may infer that AtAAN8 most likely is required for H_2O_2 distribution. This hypothesis is compatible with our observation that AtANN8-YFP associates with the ER/endomembrane in the cytoplasm (Figure 8 and Figure S3). Indeed, H_2O_2 has been reported to be produced intracellularly and transported in vesicles from an endocytic pathway to the vacuole in plant cells during salt stress response (Leshem et al. 2006). Moreover, rice OsANN1 has been shown to be involved in abiotic stress-induced production of H_2O_2 (Qiao et al. 2015). Another possibility is that like AtANN1, AtANN8 may possess peroxidase activity that allows scavenging of H_2O_2, so as to slow down the programmed cell death mediated by RPW8.1-triggerred H_2O_2.

Regardless of the mode of action, our genetic data from functional impairment or overexpression of AtANN8 (Figure 5 and Figure 6) suggest that AtANN8 may function as a stress-protectant to prevent high-level accumulation of cellular H_2O_2 triggered by RPW8.1, thereby down-regulating RPW8.1-triggered disease resistance and cell death.

Whether AtANN8 regulates other resistance genes such as RPW8.2 remains an open question. Future studies should be directed to investigating the biochemical functions of AtANN8 with regard to its potential peroxidase activity, and Ca^{2+} and lipid binding in order to understand how AtANN8 is engaged in regulation of intracellular H_2O_2 levels and/or extracellular transport of H_2O_2 during plant immune response.

MATERIALS AND METHODS

Plant materials, map-based cloning of *b7-6* and growth analysis

The transgenic line R1Y4 (at its sixth generation; Ma et al., 2014) was used for EMS-mediated mutagenesis and screening for mutants with either impaired or enhanced necrotic lesions as described in a previous report (Zhao et al. 2015). The mutant *b7-6* was isolated based on its spontaneous lesion phenotype. An F_2 population derived from crossing of *b7-6* to the Ler accession was used for mapping and identification of the causal mutation. By using 20 SSLP markers with four from each chromosome, the causal mutation was initially mapped between markers F14F18 and MYJ24 on chromosome 5 (Table S1). Based on the Cereon Genomics SNPs, new markers were developed and used to map the causal mutation in *b7-6* between T22P22 and T24H18, a region of ~340 kb covered by P1/BAC clones F14F18, MXC9 and T2L20 (Figure S1). We sequenced 9 candidate genes in this region in *b7-6* and found a G-to-A mutation that is predicted to result in an Ala94 to Thr substitution in *At5g12380*. A fragment covering *At5g12380* and its 5′-flanking sequences (promoter region) was amplified with primer pair ECOANN8-F and KPNANN8-R, and cloned into the *Eco*RI/*Bam*HI site of the binary vectors pPZP211 or *Eco*RI/*Kpn*I site of pCAMBIA1300-35S-eYFP-RBS. The resulting plasmids, pP_{ANN8}::ANN8 and pP_{ANN8}::ANN8-YFP, were introduced into *b7-6* plants for genetic complementation. SSLP markers and primers used for map-based cloning were listed in Supplementary Table S1.

To generate an *ann8-1* single mutant, R1Y4/*ann8-1* was crossed with Col-gl, and F_2 individuals homozygous for *ann8-1* was identified by a marker developed on the point mutation in *ann8-1* which led to a *Hinf*I site with primers ann8F3 and ann8R3 (Figure S1B). To over-express *AtANN8*, the *AtANN8* cDNA was amplified

with primers KPNANN8-F and SpeIANN8-R (Table S1), and cloned into *Kpn*I/*Spe*I sites of the binary vector pCAMBIA1300-35S-eYFP-RBS. The recombinant plasmid was confirmed by sequencing with primer RBS-R. Then, the construct expressing *AtANN8* under control of the constitutive promoter *35S* was introduced into the R1Y4 and Col-*gl*, respectively, via Agrobacterium-mediated transformation (Clough and Bent 1998). Positive transformants were screened on 1/2 (W/V) Murashige and Skoog (MS) medium agar plates with Hygromycin (50 mg/ml) and stable homozygous lines were identified by PCR with primers KPNANN8-F and RBS-R.

The *Arabidopsis* seeds were cold-treated at 4^{o} C for 48 h and then sown in soil (Pindstrup). Seedlings were grown under 22^{o} C, 75% RH in 8 h light and 16 h dark photo-period for 5 weeks. For plant growth in the MS agar medium, the method was used following a previous report (Xiao et al., 2003). In brief, surface-sterilized seeds were placed on MS agar medium with 100 mM NaCl, 10 μM SA, 10 μM JA, 0.1 mol H_2O_2, respectively, chilled at 4^{o} C for 48 h, then the plates were transferred to a growth room with the same conditions mentioned above.

Pathogen infection and microscopy analyses

Powdery mildew infection was performed following a previous report (Xiao *et al*., 2005). For bacterial infection analysis, *Arabidopsis* leaves were infiltrated with a suspension of the *Pst* DC3000 wild-type strain (OD_{600} = 0.0002), the avirulent strain carrying *avrRpm1*, or the *hrc*C^{-} mutant strain in H_2O.

Dead cells were examined by trypan blue staining (Xiao *et al*. 2003) at 10 dpi of powdery mildew. H_2O_2 examination *in situ* production was performed according to Xiao et al. (2003). To examine the accumulation of RPW8.1-YFP or

subcellular localization of AtANN8-YFP, leaves were examined firstly under a epi-fluorescent microscope (Nikon 80i) and then performed images acquisition using a confocal laser scanning microscope (Nikon A1, Nikon Instruments Inc. Chengdu, China) as described in a previous report (Huang et al. 2014).

Generation of *AtANN8* knockdown lines

To make an artificial microRNA (amiRNA) gene targeting *AtANN8* (*At5g12380*), gene specific primers were identified by the tool available at WMD Web MicroRNA Designer (http://wmd3.weigelworld.org). The construct expressing amiRANN8 was obtained following a previous report (Schwab et al. 2006) using the template plasmid pRS300 and primers AT5G12380miR Ⅰ, AT5G12380miR Ⅱ, AT5G12380miR Ⅲ, AT5G12380miR Ⅳ (Table 2). The resultant amiRNA was cloned into the pKANNIBAL-35S-RBS (which kindly provided by Yuelin Zhang) at *Xho*I/*Bam*HI sites. The resulting plasmid pAmiRANN8 was transformed into agrobacterium strain GV3101 together with helper plasmid pSOUP, then introduced into Col-gl via Agrobacterium-mediated floral dip (Clough and Bent 1998). The transgenic lines expressing amiRANN8 was crossed to R1Y4 to make R1Y4/*amiRANN8* lines. All primer sequences for constructs and the cloning procedures were included in Table S2.

Transcript analysis

Transcript analysis was performed following a previous report (Zhao et al. 2020a). Briefly, total RNA was extracted from ~50 mg leaves with Trizol reagent (Invitrogen). cDNA was obtained by using the SuperScript first-strand synthesis kit (Invitrogen). For time course analysis of defense genes induced by different *P. syringae* strains, inoculated leaves were collected at 0, 3, 6, 12, 24, 48 hpi and used for RNA extraction. Quantification of transcripts of *AtANN8*, *RPW8.1*, *PR1*,

and *FRK1* by reverse transcription quantitative PCR (RT-qPCR) was done as described previously (Li et al. 2014). SYBR Green mix (QuantiFast™, QIAGEN) was used in RT-qPCR to determine the abundance of mRNA. Gene expression levels were normalized by using *ACT2* as an internal control, and RT-qPCR was performed on a Bio-Rad CFX96™ Real-Time system.

Western blot assay and Co-immunoprecipitation (Co-IP) assay

Western blot assay was performed following a previous report (Zhao et al. 2020b). For Co-IP assay, *RPW8.1-HA* and *ACO4*$_{38\text{-}175}$*-Flag* constructs described in a previous report (Zhao et al. 2020b) were used. To make the *AtANN8-Flag* construct, the coding sequence of At*ANN8* was amplified from the cDNA of R1Y4 with the primers shown in Table S2. The Flag epitope tag was translationally fused with *AtANN8* at its 3' end to make *ANN8-Flag*. Then, RPW8.1-HA was transiently co-expressed with ANN8-Flag or ACO4$_{38\text{-}175}$-Flag in leaves of *N. benthamiana*. Total protein extracted from the infiltrated *N. benthamiana* leaves was subjected to Co-IP as described in a previous report (Zhao et al. 2020b).

Acknowledgments

This work was supported by the National Natural Science Foundation of China (Grant numbers 31672090, 31430072 and 31371931 to W.-M.W.) and the National Science Foundation (Grant numbers IOS-1457033 and IOS-1901566 to S.X.). We thank Dr. Yuelin Zhang (The University of British Columbia) for the vector pKANNIBAL-35S-RBS, Ling-Li Zhang (Rice Research Institute, Sichuan Agricultural University) for technique support.

AUTHOR CONTRIBUTIONS

Z.-X.Z., Y.-J.X., Y.L., and Q.L. performed the experiments with support from J.-Q.Z., Y.L., J.F., S.X. and W.-M.W. S.X. and W.-M.W. conceived the project. W.-M.W designed the experiments. Z.-X.Z., and W.-M.W. analyzed the data and wrote the manuscript. All authors read and approved of this content. The authors declare no conflict of interest.

REFERENCES

Bittel P, Robatzek S (2007) Microbe-associated molecular patterns (MAMPs) probe plant immunity. **Curr Opin Plant Biol** 10: 335-341

Brueggeman R, Rostoks N, Kudrna D, Kilian A, Han F, Chen J, Druka A, Steffenson B, Kleinhofs A (2002) The barley stem rust-resistance gene Rpg1 is a novel disease-resistance gene with homology to receptor kinases. **Proc Natl Acad Sci U S A** 99: 9328-9333

Castel B, Ngou P-M, Cevik V, Redkar A, Kim D-S, Yang Y, Ding P, Jones JDG (2019) Diverse NLR immune receptors activate defence via the RPW8-NLR NRG1. **New phytologist** 222: 966-980

Chandran D, Inada N, Hather G, Kleindt CK, Wildermuth MC (2010) Laser microdissection of Arabidopsis cells at the powdery mildew infection site reveals site-specific processes and regulators. **Proc Natl Acad Sci U S A** 107: 460-465

Clough SJ, Bent AF (1998) Floral dip: a simplified method for Agrobacterium-mediated transformation of Arabidopsis thaliana. **Plant J** 16: 735-743

Dangl JL, Horvath DM, Staskawicz BJ (2013) Pivoting the plant immune system from dissection to deployment. **Science** 341: 746-751

Dodds PN, Rathjen JP (2010) Plant immunity: towards an integrated view of plant-pathogen interactions. **Nat Rev Genet** 11: 539-548

Dou D, Zhou JM (2012) Phytopathogen effectors subverting host immunity: different foes, similar battleground. **Cell Host Microbe** 12: 484-495

Espinoza C, Liang Y, Stacey G (2017) Chitin receptor CERK1 links salt stress and chitin-triggered innate immunity in Arabidopsis. **Plant J** 89: 984-995

Gerke V, Creutz CE, Moss SE (2005) Annexins: linking Ca2+ signalling to membrane dynamics. **Nat Rev Mol Cell Biol** 6: 449-461

Gidrol X, Sabelli PA, Fern YS, Kush AK (1996) Annexin-like protein from Arabidopsis thaliana rescues delta oxyR mutant of Escherichia coli from H2O2 stress. **Proc Natl Acad Sci U S A** 93: 11268-11273

Gorantla M, Babu PR, Lachagari VBR, Feltus FA, Paterson AH, Reddy AR (2005) Functional genomics of drought stress response in rice: transcript mapping of annotated unigenes of an indica rice (*Oryza sativa* L. cv. Nagina 22). **Curr. Sci.** 89: 496-514

Huang Y-Y, Zhang L-L, Ma X-F, Zhao Z-X, Zhao J-H, Zhao J-Q, Fan J, Li Y, He P, Xiao S, Wang W-M (2019) Multiple intramolecular trafficking signals in RESISTANCE TO POWDERY MILDEW 8.2 are engaged in activation of cell death and defense. **Plant J** 98: 55-70

Huang YY, Shi Y, Lei Y, Li Y, Fan J, Xu YJ, Ma XF, Zhao JQ, Xiao S, Wang WM (2014) Functional identification of multiple nucleocytoplasmic trafficking signals in the broad-spectrum resistance protein RPW8.2. **Planta** 239: 455-468

Huh SM, Noh EK, Kim HG, Jeon BW, Bae K, Hu HC, Kwak JM, Park OK (2010) Arabidopsis annexins AnnAt1 and AnnAt4 interact with each other and regulate drought and salt stress responses. **Plant Cell Physiol** 51: 1499-1514

Jami SK, Clark GB, Turlapati SA, Handley C, Roux SJ, Kirti PB (2008) Ectopic expression of an annexin from Brassica juncea confers tolerance to abiotic and biotic stress treatments in transgenic tobacco. **Plant Physiol Biochem** 46: 1019-1030

Jones JD, Dangl JL (2006) The plant immune system. **Nature** 444: 323-329

Konopka-Postupolska D, Clark G, Goch G, Debski J, Floras K, Cantero A, Fijolek B, Roux S, Hennig J (2009) The role of annexin 1 in drought stress in Arabidopsis. **Plant Physiol** 150: 1394-1410

Krattinger SG, Lagudah ES, Spielmeyer W, Singh RP, Huerta-Espino J, McFadden H, Bossolini E, Selter LL, Keller B (2009) A putative ABC transporter confers durable resistance to multiple fungal pathogens in wheat. **Science** 323: 1360-1363

Laohavisit A, Brown AT, Cicuta P, Davies JM (2010) Annexins: components of the calcium and reactive oxygen signaling network. **Plant Physiol** 152: 1824-1829

Laohavisit A, Davies JM (2011) Annexins. **New Phytol** 189: 40-53

Laohavisit A, Mortimer JC, Demidchik V, Coxon KM, Stancombe MA, Macpherson N, Brownlee C, Hofmann A, Webb AA, Miedema H, Battey NH, Davies JM (2009) Zea mays annexins modulate cytosolic free Ca2+ and generate a Ca2+-permeable conductance. **Plant Cell** 21: 479-493

Laohavisit A, Shang Z, Rubio L, Cuin TA, Very AA, Wang A, Mortimer JC, Macpherson N, Coxon KM, Battey NH, Brownlee C, Park OK, Sentenac H, Shabala S, Webb AA, Davies JM (2012) Arabidopsis annexin1 mediates the radical-activated plasma membrane Ca(2)+- and K+-permeable conductance in root cells. **Plant Cell** 24: 1522-1533

Leshem Y, Melamed-Book N, Cagnac O, Ronen G, Nishri Y, Solomon M, Cohen G, Levine A (2006) Suppression of Arabidopsis vesicle-SNARE expression inhibited fusion of H2O2-containing vesicles with tonoplast and increased salt tolerance. **Proc Natl Acad Sci U S A** 103: 18008-18013

Li Y, Huang F, Lu Y, Shi Y, Zhang M, Fan J, Wang W (2013) Mechanism of plant-microbe interaction and its utilization in disease-resistance breeding for modern agriculture. **Physiological and Molecular Plant Pathology** 83: 51-58

Li Y, Lu YG, Shi Y, Wu L, Xu YJ, Huang F, Guo XY, Zhang Y, Fan J, Zhao JQ, Zhang HY, Xu PZ, Zhou JM, Wu XJ, Wang PR, Wang WM (2014) Multiple rice microRNAs are involved in immunity against the blast fungus Magnaporthe oryzae. **Plant Physiol** 164: 1077-1092

Li Y, Zhang Y, Wang Q-X, Wang T-T, Cao X-L, Zhao Z-X, Zhao S-L, Xu Y-J, Xiao Z-Y, Li J-L, Fan J, Yang H, Huang F, Xiao S, Wang W-M (2018) RESISTANCE TO POWDERY MILDEW8.1 boosts pattern-triggered immunity against multiple pathogens in Arabidopsis and rice. **Plant Biotechnol J** 16: 428-441

Ma XF, Li Y, Sun JL, Wang TT, Fan J, Lei Y, Huang YY, Xu YJ, Zhao JQ, Xiao S, Wang WM (2014) Ectopic expression of RESISTANCE TO POWDERY MILDEW8.1 confers resistance to fungal and oomycete pathogens in Arabidopsis. **Plant Cell Physiol** 55: 1484-1496

Meers P, Mealy T (1994) Phospholipid determinants for annexin V binding sites and the role of tryptophan 187. **Biochemistry** 33: 5829-5837

Nirmala J, Drader T, Lawrence PK, Yin C, Hulbert S, Steber CM, Steffenson BJ, Szabo LJ, von Wettstein D, Kleinhofs A (2011) Concerted action of two avirulent spore effectors activates Reaction to Puccinia graminis 1 (Rpg1)-mediated cereal stem rust resistance. **Proc Natl Acad Sci U S A** 108: 14676-14681

Orgil U, Araki H, Tangchaiburana S, Berkey R, Xiao S (2007) Intraspecific genetic variations, fitness cost and benefit of RPW8, a disease resistance locus in Arabidopsis thaliana. **Genetics** 176: 2317-2333

Qiao B, Zhang Q, Liu D, Wang H, Yin J, Wang R, He M, Cui M, Shang Z, Wang D, Zhu Z (2015) A calcium-binding protein, rice annexin OsANN1, enhances heat stress tolerance by modulating the production of H2O2. **J Exp Bot** 66: 5853-5866

Richards SL, Laohavisit A, Mortimer JC, Shabala L, Swarbreck SM, Shabala S, Davies JM (2014) Annexin 1 regulates the H2O2-induced calcium signature in Arabidopsis thaliana roots. **Plant J** 77: 136-145

Risk JM, Selter LL, Chauhan H, Krattinger SG, Kumlehn J, Hensel G, Viccars LA, Richardson TM, Buesing G, Troller A, Lagudah ES, Keller B (2013) The wheat Lr34 gene provides resistance against multiple fungal pathogens in barley. **Plant Biotechnol J** 11: 847-854

Schwab R, Ossowski S, Riester M, Warthmann N, Weigel D (2006) Highly specific gene silencing by artificial microRNAs in Arabidopsis. **Plant Cell** 18: 1121-1133

Seybold H, Trempel F, Ranf S, Scheel D, Romeis T, Lee J (2014) Ca2+ signalling in plant immune response: from pattern recognition receptors to Ca2+ decoding mechanisms. **New Phytol** 204: 782-790

Truman W, Bennett MH, Kubigsteltig I, Turnbull C, Grant M (2007) Arabidopsis systemic immunity uses conserved defense signaling pathways and is mediated by jasmonates. **Proc Natl Acad Sci U S A** 104: 1075-1080

Wang W, Berkey R, Wen Y, Xiao S (2010) Accurate and adequate spatiotemporal expression and localization of RPW8.2 is key to activation of resistance at the host-pathogen interface. **Plant Signal Behav** 5: 1002-1005

Wang W, Wen Y, Berkey R, Xiao S (2009) Specific targeting of the Arabidopsis resistance protein RPW8.2 to the interfacial membrane encasing the fungal Haustorium renders broad-spectrum resistance to powdery mildew. **Plant Cell** 21: 2898-2913

Wang W, Yang X, Tangchaiburana S, Ndeh R, Markham JE, Tsegaye Y, Dunn TM, Wang GL, Bellizzi M, Parsons JF, Morrissey D, Bravo JE, Lynch DV, Xiao S (2008) An inositolphosphorylceramide synthase is involved in regulation of plant programmed cell death associated with defense in Arabidopsis. **Plant Cell** 20: 3163-3179

Wang WM, Ma XF, Zhang Y, Luo MC, Wang GL, Bellizzi M, Xiong XY, Xiao SY (2012) PAPP2C interacts with the atypical disease resistance protein RPW8.2 and

negatively regulates salicylic acid-dependent defense responses in Arabidopsis. **Mol Plant** 5: 1125-1137

Wang X, Ma X, Wang H, Li B, Clark G, Guo Y, Roux S, Sun D, Tang W (2015) Proteomic study of microsomal proteins reveals a key role for Arabidopsis annexin 1 in mediating heat stress-induced increase in intracellular calcium levels. **Mol Cell Proteomics** 14: 686-694

Wang Y, Ohara Y, Nakayashiki H, Tosa Y, Mayama S (2005) Microarray analysis of the gene expression profile induced by the endophytic plant growth-promoting rhizobacteria, Pseudomonas fluorescens FPT9601-T5 in Arabidopsis. **Mol Plant Microbe Interact** 18: 385-396

Wu Z, Li M, Dong OX, Xia S, Liang W, Bao Y, Wasteneys G, Li X (2019) Differential regulation of TNL-mediated immune signaling by redundant helper CNLs. **New phytologist** 222: 938-953

Xiao S, Brown S, Patrick E, Brearley C, Turner JG (2003) Enhanced transcription of the Arabidopsis disease resistance genes RPW8.1 and RPW8.2 via a salicylic acid-dependent amplification circuit is required for hypersensitive cell death. **Plant Cell** 15: 33-45

Xiao S, Ellwood S, Calis O, Patrick E, Li T, Coleman M, Turner JG (2001) Broad-spectrum mildew resistance in Arabidopsis thaliana mediated by RPW8. **Science** 291: 118-120

Zhao Z-X, Feng Q, Cao X-L, Zhu Y, Wang H, Chandran V, Fan J, Zhao J-Q, Pu M, Li Y, Wang W-M (2020a) Osa-miR167d facilitates infection of Magnaporthe oryzae in rice. **J Integr Plant Biol** 62: 702-715

Zhao Z-X, Feng Q, Liu P-Q, He X-R, Zhao J-H, Xu Y-J, Zhang L-L, Huang Y-Y, Zhao J-Q, Fan J, Li Y, Xiao S, Wang W-M (2020b) RPW8.1 enhances the ethylene signaling pathway to feedback attenuate its mediated cell death and disease resistance in Arabidopsis. **New phytologist** n/a:

Zhao Z-X, Xu Y-B, Wang T-T, Ma X-F, Zhao J-Q, Li Y, Fan J, Wang W-M (2015) Proper expression of AS1 is required for RPW8.1-mediated defense against powdery mildew in Arabidopsis. **Physiological and Molecular Plant Pathology** 92: 101-111

Zhou J-M, Zhang Y (2020) Plant Immunity: Danger Perception and Signaling. **Cell** 181: 978-989

Zhou ML, Yang XB, Zhang Q, Zhou M, Zhao EZ, Tang YX, Zhu XM, Shao JR, Wu YM (2013) Induction of annexin by heavy metals and jasmonic acid in Zea mays. **Funct Integr Genomics** 13: 241-251

Figure legends

Figure 1. Isolation of the *RPW8.1* enhancer mutant *b7-6* and identification of the causal mutation

(**A**) Representative plants of the indicated lines showing the phenotype of R1Y4 and *b7-6*. (**B**) Representative leaves from the indicated lines showing the pits in R1Y4 (arrowheads) and spontaneous HR-like lesions in *b7-6* (arrows). (**C**) Schematic gene structure of *AtANN8* (*At5g12380*) and the position of the causal mutation in *b7-6*. P1 and P2 indicate the position of primers for RT-PCR and reverse transcription quantitative PCR (RT-qPCR). The red box indicates target site of the artificial microRNA gene designed. (**D**) Predicted protein structure of AtANN8 and the amino acid substitution site in *b7-6*. ANX, ANNEXIN domain. (**E**) Alignment of the region between the first two ANX domains from predicted plant and animal ANN8-like protein sequences. Identical residues are highlighted in yellow as red letters. Ala at position 94 of AtANN8, which is substituted by Thr (*) in *b7-6*, is underlined at the consensus. (**F**) Representative leaves from the indicated lines showing genetic complementation of *b7-6* with AtANN8-YFP expressed from its native promoter. Sequence data in (E) can be found in the GenBank/EMBL databases or *Arabidopsis* Genome Initiative under the following accession numbers: *Oryza sativa* Japonica NP_001055408; *Theobroma cacao* (cacao) EOY32842; *Cucumis sativus* (cucumber) XP_004139124; *Vitis vinifera* (wine grape) XP_002279669; *Gossypium hirsutum* (upland cotton) ACJ11719; *Prunus persica* (peach) EMJ19904; *Nicotiana tabacum* (common tobacco) AAX78200; *Glycine max* (soybean) XP_003546292; *Aegilops* EMT22984; *Drosophila melanogaster* (fruit fly) NP_996253; *Mus musculus* (house mouse)

NP_081487; *Homo sapiens* (human) NP_004297; AtANN8 At5g12380 (CAC42899).

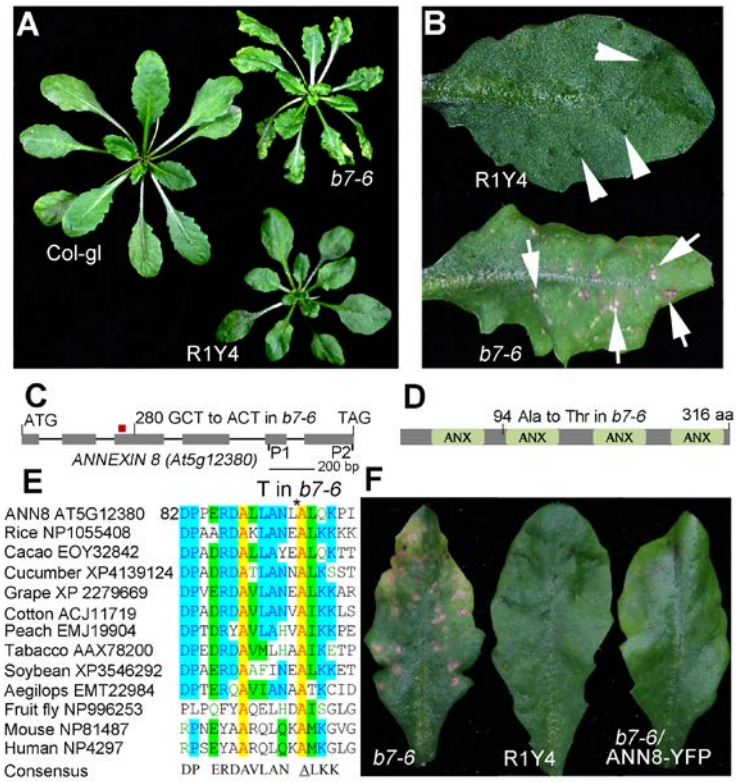

Figure 2. Differential responses of *ANNEXIN* genes to pathogen infection

(**A**-**E**) Expression of indicated genes in the indicated plant tissues (**A**) or in leaves collected at the indicated time points after inoculation of the indicated *P. syringae* strains with H_2O as control (**B**-**E**). RNA was extracted from the indicated tissues (**A**) or from leaves at the indicated time points (**B**-**E**) for reverse transcription quantitative PCR (RT-qPCR) analysis. mRNA level was normalized to that in stem (**A**) or to that in H_2O (0 hpi) (**B**-**E**). Error bars indicate *SD* ($n = 3$). Student's *t* test was carried out to determine the significance of differences between naïve leaves and mildew-infected leaves (**A)** or between H_2O-treated leaves and leaves inoculated with bacterial pathogens at the same time point (**B**-**E**). Asterisks * and ** indicate significant differences at $P < 0.05$ and $P < 0.01$, respectively. Note that *AtANN8* was preferentially expressed in leaves relative to stem and flower tissues and up-regulated at 10 days post inoculation of the powdery mildew pathogen *Golovinomyces cichoracearum* UCSC1.

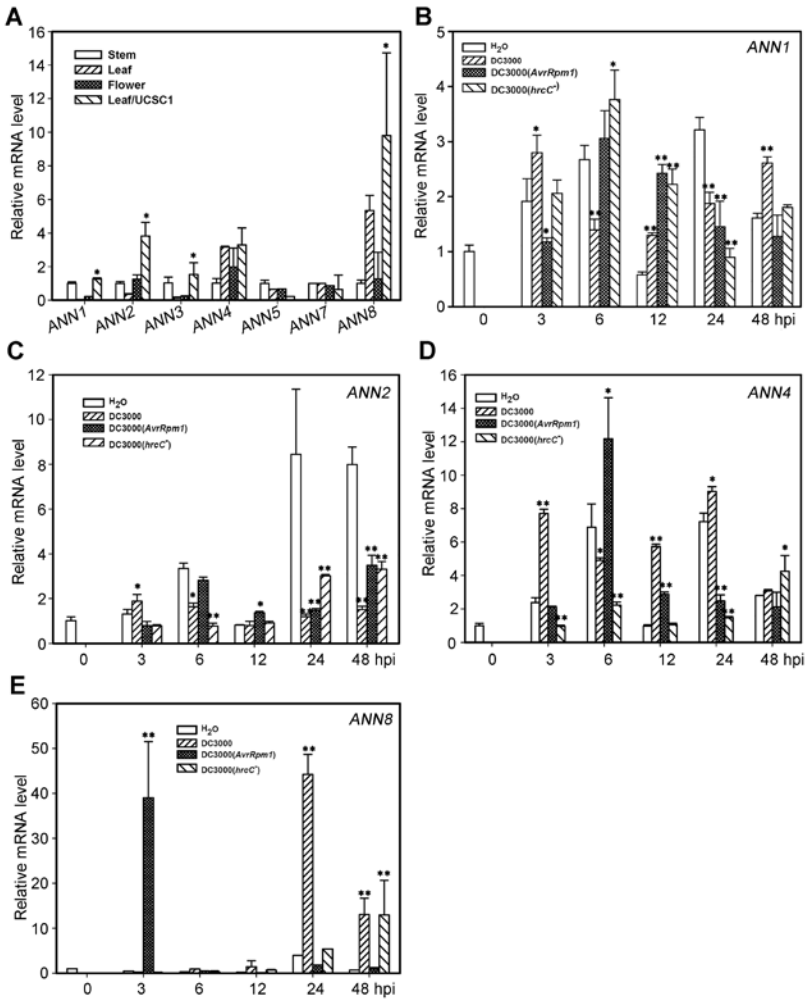

Figure 3. Silencing of *AtANN8* leads to RPW8.1-dependent necrotic lesions

(**A**) Representative leaves from the indicated lines showing that *ann8-1* alone did not have necrotic lesions as in R1Y4/*ann8-1*. (**B**) Growth of the virulent bacterial strain *Pseudomonas syringe* DC3000 in the indicated lines at the indicated time points. Error bars indicate *SD* (n = 4). Different letters above the bars indicate significant differences ($P < 0.05$) determined by One-way ANOVA. (**C**) A representative leaf from Col-gl compared with representative leaves from the indicated lines expressing artificial microRNA (amiRANN8) targeting *AtANN8*. (**D**) Comparison of the *AtANN8* expression in the indicated lines detected by RT-qPCR with that in Col-gl, which is set to 1. Different letters indicate significant differences ($P < 0.01$) determined by One-way ANOVA. (**E**) Representative leaves from the indicated lines showing that knocking-down of *AtANN8* by *amiRANN8* in the R1Y4 background led to necrotic lesions (arrows) similar to those seen in R1Y4/*ann8-1*.

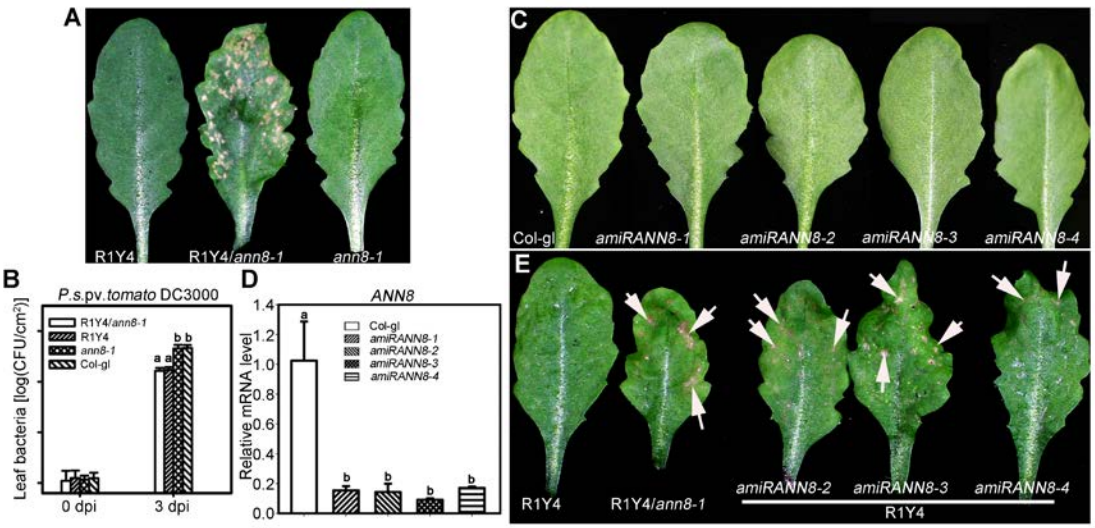

Figure 4. Functional impairment of *AtANN8* up-regulates *RPW8.1* expression and enhanced RPW8.1-mediated disease resistance

(**A**-**C**) Confocal micrographs showing the accumulation of RPW8.1-YFP in R1Y4 (**A**), R1Y4/*ann8-1* (**B**) and R1Y4/*amiRANN8-3* (**C**). YFP fluorescence is presented in green and auto-fluorescence of chloroplasts is in red. Size bar, 20 μm. (**D** and **E**) Fluorescent intensity in the indicated lines measured by Image J from confocal micrographs and expression of *RPW8.1* in indicated lines measured by RT-qPCR. Error bars indicate *SD* (n = 3). Student's t test was carried out to determine the significance between R1Y4 and R1Y4/*ann8-1* or R1Y4/*amiRANN8-3*, respectively. Asterisk * indicates significant differences at $P < 0.01$. (**F**) Representative leaves from the indicated lines showing the disease phenotypes at 10 dpi with *G. cichoracearum* UCSC1. (**G**) Quantification of *G. cichoracearum* UCSC1 sporulation on leaves of the indicated lines at 10 dpi. Values are means of three replications. Error bars indicate SD. Different letters above the bars indicate significant differences ($P < 0.01$) determined by One-way ANOVA. (**H** and **I**) Expression of the PTI marker gene *FRK1* (H) and the SA-pathway defense marker gene *PR1* (**I**) at the indicated time points from the indicated lines evaluated by reverse transcription quantitative PCR (RT-qPCR) analysis. Error bars indicate *SD* (n = 3). Student's t-test was carried out to determine the significance between R1Y4 and R1Y4/*ann8-1* at the same time point. Asterisks * and ** indicate significant differences at $P < 0.05$ and $P < 0.01$, respectively.

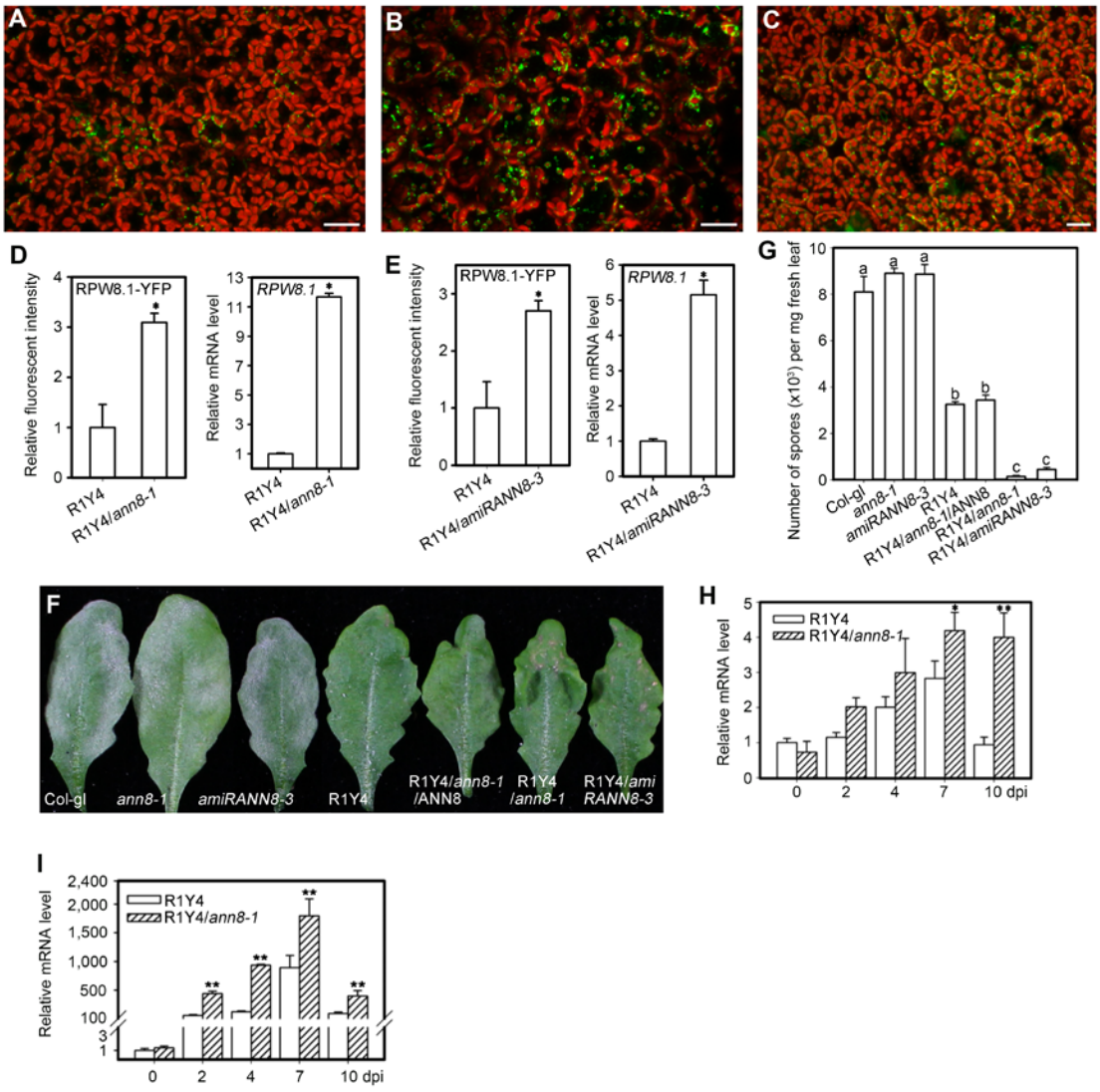

Figure 5. Mutation in *AtANN8* results in enhanced RPW8.1-mediated cell death and altered RPW8.1-triggered H_2O_2 pattern

(**A**-**D**) Trypan blue-stained leaves (**A** and **C**) and leaf sections (**B** and **D**) free of pathogen infection (**A** and **B**) and at 10 dpi of *G. cichoracearum* UCSC1 (**C** and **D**) from the indicated lines. Dying/dead cells are stained blue by Trypan blue. Size bar, 50 μm. (**E** and **F**) Micrographs showing 3,3'-diaminobenzidine (DAB) stained H_2O_2 accumulation pattern in R1Y4. Note that H_2O_2 was distributed in apoplastic space with no cell-shape change (**E**) or surrounded by oval-shaped mesophyll cells (*)(**F**). (**G** and **H)** Micrographs showing DAB stained H_2O_2 accumulation pattern in R1Y4/*ann8-1*. White asterisk indicates the shrunken cytoplasm in a dying cell (**G**). Arrowheads indicate H_2O_2 in chloroplasts. Arrows indicate H_2O_2-containing objects in the extracellular space (**H**). Size bar, 20 μm.

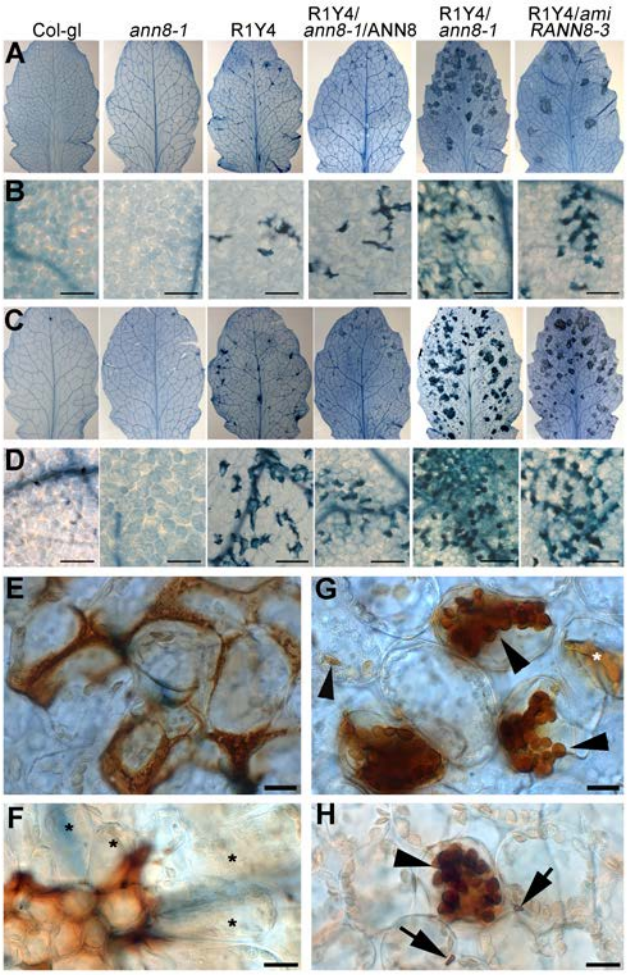

Figure 6. Over-expression of *AtANN8* compromises *RPW8.1*-mediated disease resistance

(**A**) A comparison of leaves from the indicated lines, showing pits (arrowheads) only in a leaf from R1Y4. (**B** and **C**) Expression of *AtANN8* (**B**) and *RPW8.1* (**C**) from the indicated lines examined by reverse transcription quantitative PCR (RT-qPCR). Error bars indicate *SD* (n = 3). Student's t test was carried out to determine the significance of differences between Col-gl and the other lines (**B**) or between R1Y4 and the other lines (**C**). Asterisks * and ** indicate significant differences at $P < 0.01$ and $P < 0.0001$, respectively. Values above the bars indicate transcripts abundance of *AtANN8* (**B**) and *RPW8.1* (**C**) in the indicated lines relative to that in the control lines, which were set to 1.0. (**D**) Representative leaves from the indicated lines showing the disease phenotypes at 10 dpi of *G. cichoracearum*. (**E**) Quantification of *G. cichoracearum* sporulation on leaves of the indicated lines at 10 dpi. Values are means of three replications. Error bars indicate SD. Different letters indicate significant differences ($P < 0.01$) determined by One-way ANOVA.

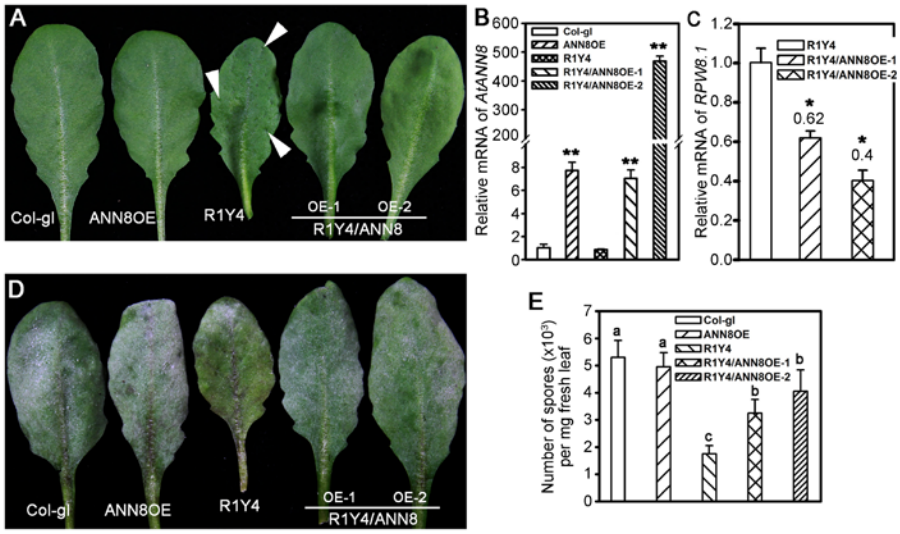

Figure 7. AtANN8 is required for adaptation to salt stress

(**A**) Seedlings from the indicated lines at 10 d after transfer to control (H_2O) or test plates. Note that the A94T missense mutation in AtANN8 (*ann8-1*) led to hypersensitivity to salt stress as shown by the shorter roots in NaCl media, and hyposensitivity to SA as shown by the longer roots in SA media. (**B**) Root inhibition assays of the indicated lines grown on media containing four different chemicals, each of which was normalized to root growth in the control plates. Error bars indicate *SD* (n = 3). Student's t test was carried out to determine the significance of differences between Col-gl and the *AtANN8* mutant lines. Asterisk * indicates significant differences at $P < 0.01$.

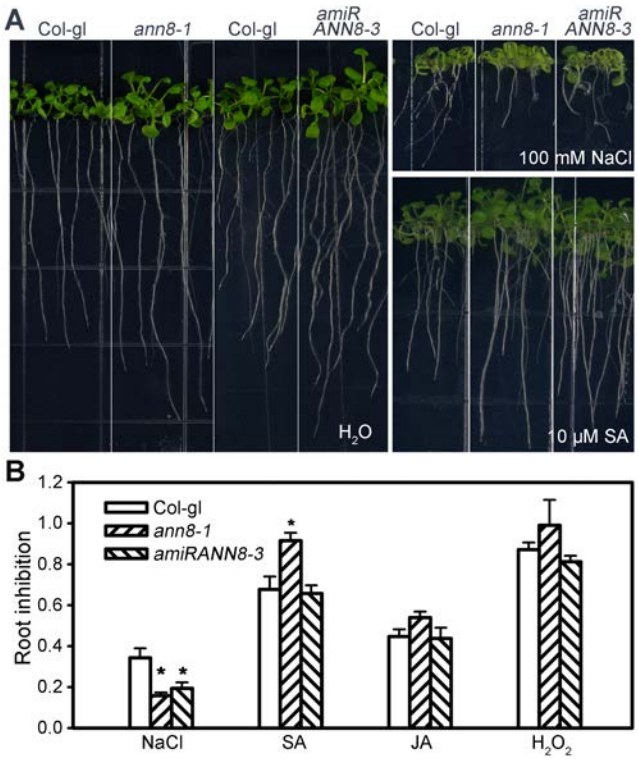

Figure 8. AtANN8 is localized at the endoplasmic reticulum (ER)

(**A**) A representative confocal image showing the localization pattern of AtANN8-YFP expressed from the native promoter in a stable transgenic *Arabidopsis* plant. Arrows indicate intracellular structure. (**B** and **C**) Representative confocal images showing co-localization between AtANN8-YFP and the ER marker 2RFP-HDEL transiently co-expressed in leaves of *N. benthamiana*. Arrow indicates the nucleus. Size bar, 10 μm.